Available online at www.sciencedirect.com
SCIENCE DIRECT
Journal of Colloid and Interface Science 298 (2006) 973–981
JOURNAL OF Colloid and Interface Science
www.elsevier.com/locate/jcis

Dependence of the broad frequency dielectric spectra of colloidal polystyrene particle suspensions on the difference between the counterion and co-ion diffusion coefficients

Mónica Tirado [a], Constantino Grosse [a,b,*]

[a] *Departamento de Física, Universidad Nacional de Tucumán, Av. Independencia 1800, (4000) San Miguel de Tucumán, Argentina*
[b] *Consejo Nacional de Investigaciones Científicas y Técnicas, Argentina*

Received 6 December 2005; accepted 12 January 2006

Available online 7 February 2006

Abstract

Dielectric properties of four suspensions of spherical polystyrene particles were measured at 25 °C over a broad frequency range extending from 100 Hz to 10 MHz, using a HP 4192 A Impedance Analyzer. The instrument was coupled to a cell with parallel platinum black electrodes and variable spacing, and the quadrupole calibration method was used. The aqueous electrolyte solutions were prepared using equal concentrations of NaCl, KCl, NaAc, or KAc, so that the calculated Debye screening length and Zeta potential remained constant, while the conductivity changed. The polystyrene particles used (Interfacial Dynamics Corp., surfactant-free white sulfate latex) have a diameter of 1 micron and a surface charge density that is independent of the pH. The dielectric spectra were described using the Nettelblad–Niklasson expression combined with a Debye type high-frequency term and analyzed using the Shilov–Dukhin theory and numerical results. The theoretical prediction that the low-frequency dispersion parameters are determined by the co-ion diffusion coefficient was experimentally confirmed. This also allowed to justify an alternative definition of the characteristic time of the low-frequency dispersion. On the contrary, the prediction that the high-frequency dispersion parameters are determined by the diffusion coefficient of counterions could not be confirmed, possibly due to experimental problems. However, the ζ-potential values deduced from high-frequency data were compatible with values deduced from electrophoretic mobility measurements.

Keywords: Dielectric dispersion; Diffusion coefficients; Colloidal suspensions; Polystyrene particles; Counterions; Co-ions; Dielectric spectroscopy; Permittivity; Conductivity

1. Introduction

The frequency behavior of the dielectric properties of aqueous suspensions of charged spherical monodispersed particles was widely studied experimentally [1–7], theoretically [8–12] and numerically [13–15]. Most of the studies deal with the dependence of the dielectric spectra on the particle size, particle concentration, particle charge, electrolyte concentration, and pH. However, except for a few recent experimental [16], theoretical [17], and numerical [18–20] studies, there is little information about the dependence on the difference between the counterion and co-ion diffusion coefficients.

In this work we analyze this dependence considering four suspensions that are identical in all respects except for the electrolytes used: potassium acetate (KAc), sodium acetate (NaAc), potassium chloride (KCl), and sodium chloride (NaCl). These particular salts were chosen in order to get symmetrical and non-symmetrical systems, in what concerns the ion diffusion coefficient values, Fig. 1. Moreover, since for each counterion (K^+ and Na^+) there are two possible co-ions (Ac^- and Cl^-), and vice versa, this set should suffice to determine the spectral properties that are mainly determined by the counterions or the co-ions in the system.

We present experimental data, measured in a broad frequency range covering both the low- and the high-frequency dispersions. This data is first described using a spectral func-

* Corresponding author.
E-mail address: cgrosse@herrera.unt.edu.ar (C. Grosse).

0021-9797/$ – see front matter
doi:10.1016/j.jcis.2006.01.027

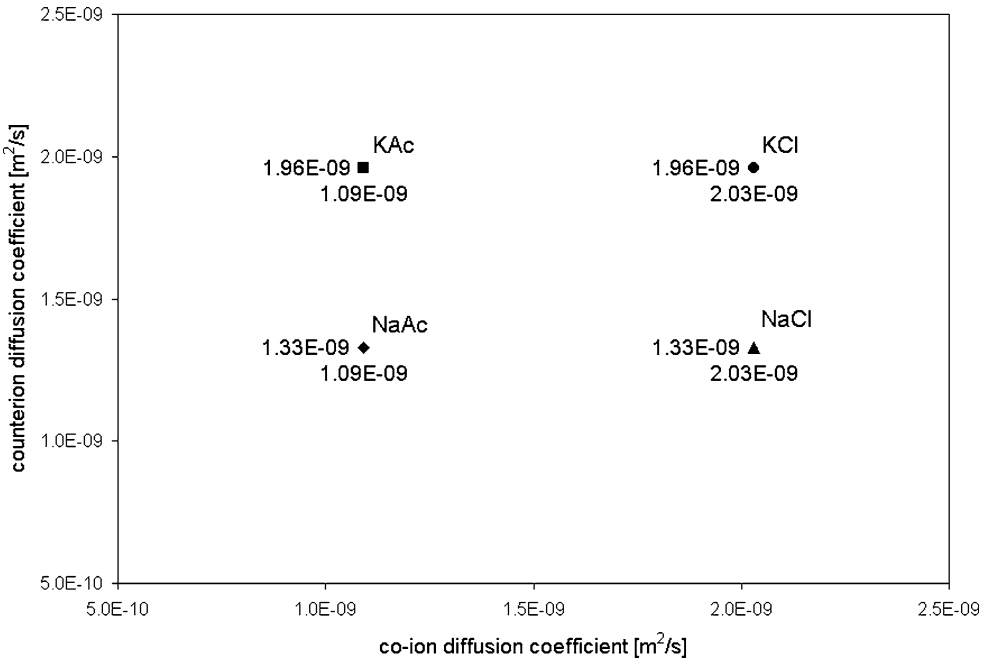

Fig. 1. Diffusion coefficients of counterions and co-ions present in the four studied suspensions.

tion and then analyzed using theoretical results, which are in turn verified with the help of numerical calculations.

2. Materials and methods

Four suspensions of monodisperse latex particles suspended in aqueous electrolyte solutions were prepared. They all contained a volume concentration $\phi = 0.01$ of surfactant-free white sulfate latex particles (Interfacial Dynamics Corp.), which have a nominal radius $a = 0.5$ μm with a 0.012 μm standard deviation, and a pH independent surface charge density of 7.6 μC/cm^2. The number concentration $C_\infty = 1.765 \times 10^{23}$ m^{-3} of counterions or co-ions in the suspending medium was also the same, and the only difference was in the electrolytes used: KAc, NaAc, KCl, or NaCl.

The electrolyte solutions were prepared using bidistilled and deionized water, while the different salts: KAc (J.T. Baker), NaAc (Timper), KCl (Cicarelli), and NaCl (Mallinckrodt), were used without further purification. The particles, supplied as a 8.2 ± 0.1 g/100 ml suspension in distilled deionized water were also used without further purification.

For the four suspensions, the value of the product κa, where κ is the reciprocal Debye length

$$\kappa = \sqrt{\frac{2e^2 C_\infty}{\varepsilon_0 \varepsilon_e kT}},$$

had the same value 28.1, calculated for the temperature of the measurements ($25 \pm 0.2\,^\circ$C). In this expression, e is the elementary charge, k the Boltzmann constant, T the absolute temperature, ε_0 the absolute permittivity of free space, and ε_e the relative permittivity of the electrolyte solution. On the contrary, the conductivities of the suspending media:

$$\sigma_e = \frac{e^2 C_\infty}{kT}\left(D^+ + D^-\right), \tag{1}$$

where D^+ and D^- are the diffusion coefficients of counterions and co-ions, varied in the 0.00351 S/m (for NaAc) to 0.00554 S/m (for KCl) range.

Impedance spectroscopy measurements were made in the 100 Hz to 10 MHz frequency range using a Hewlett Packard 4192A Impedance Analyzer under computer control. The measurement cell is a Plexiglas cylinder with flat 15 mm diameter electrodes and variable spacing that can be continuously adjusted between 0 and 9 mm [21]. The platinum electrodes, coated with platinum black, are connected to the instrument by means of coaxial cables in the Five–Terminal Pair configuration (5T) [22]. All the measurements were performed using the same pair of electrodes that were platinized prior to each measurement. In view of the low conductivity of the samples ($\sigma_s(0) \approx 0.005$ S/m) the spacing was reduced to minimize stray field effects: between 3 and 1 mm in 0.5 mm intervals [21]. The calibration of the instrument was made using the quadrupolar method [23] that complements the standard short and open calibration with a third calibration using the cell filled with an electrolyte solution with known dielectric properties as a load.

These measurements were complemented with determinations of the pH of the suspensions using a PerpHecT model 370 meter. The electrophoretic mobility of the particles was measured in highly dilute suspensions ($\phi \approx 10^{-4}$) prepared with the four electrolyte solutions (KAc, NaAc, KCl, or NaCl), using a Malvern Zeta-Sizer 2000 (Malvern Instruments, UK).

3. Experimental results

The experimental results for the relative permittivity $\varepsilon_s(\omega)$ and conductivity $\sigma_s(\omega)$ spectra of the four studied suspensions appear in Figs. 2–5. They clearly show two dispersion regions. Due to the large size of the particles and to the low conductivity of the electrolyte solutions, the low- and the high-frequency

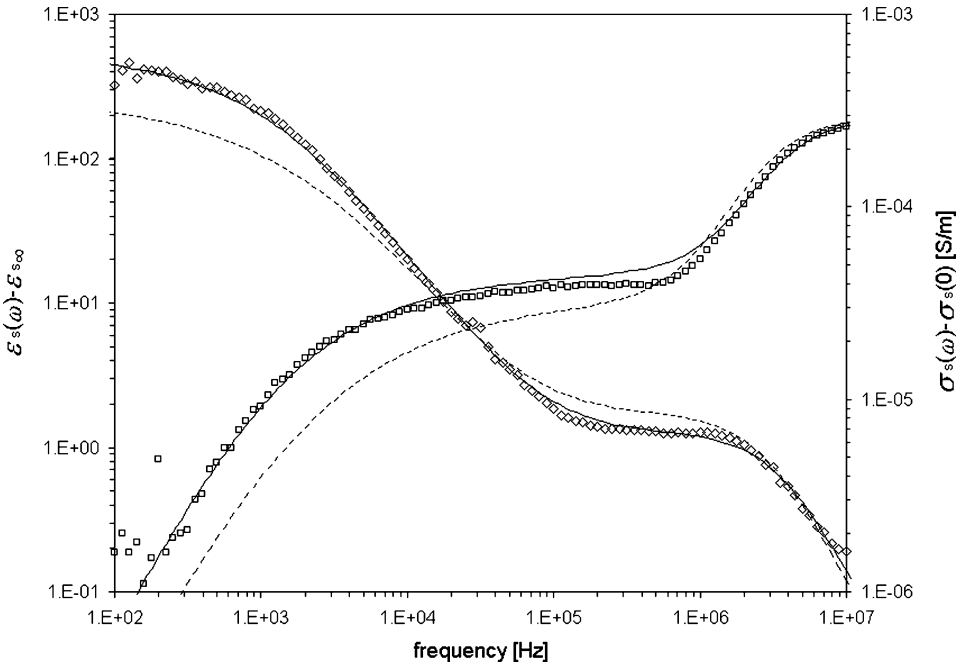

Fig. 2. Permittivity and conductivity spectra for a suspension of latex particles in aqueous KAc electrolyte solution. Theoretical values (dashed lines), fitted values (solid lines), experimental permittivity (squares) and conductivity (diamonds) data.

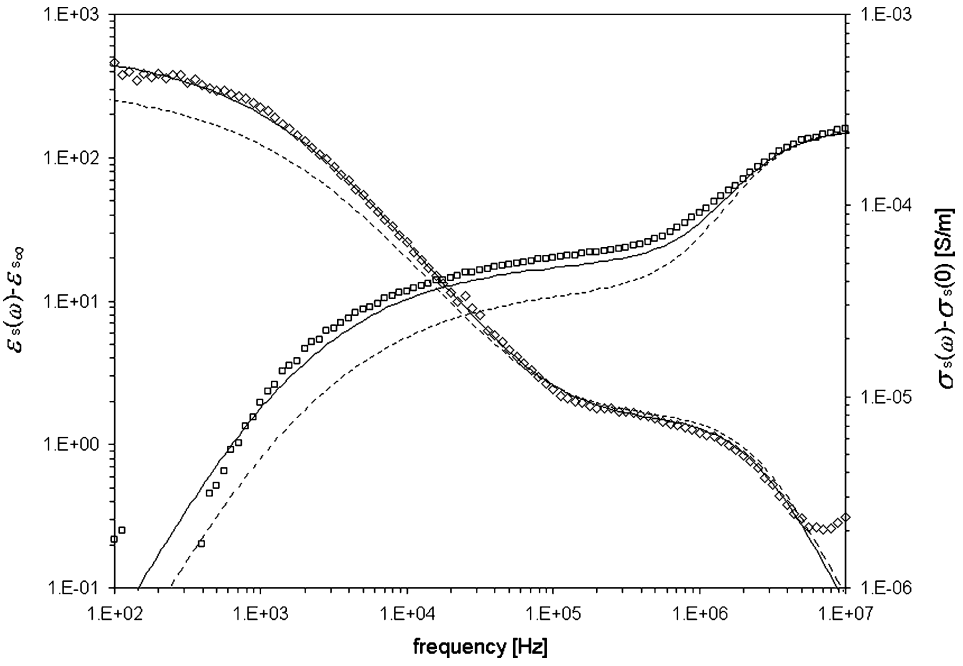

Fig. 3. As Fig. 2 but for a NaAc electrolyte solution.

dispersions are well separated and fit inside the frequency range of the measurements. Note that the plotted quantities are actually $\varepsilon_s(\omega) - \varepsilon_{s\infty}$ and $\sigma_s(\omega) - \sigma_s(0)$, where $\varepsilon_{s\infty}$ and $\sigma_s(0)$ are the limiting high-frequency permittivity and low-frequency conductivity of the suspensions. This particular representation made it possible to use logarithmic scales, expanding the otherwise invisible high-frequency permittivity and low-frequency conductivity dispersions.

The strong permittivity increase at low frequencies corresponds to the alpha dispersion. The variable spacing technique [24], combined with a Short-Open-Load calibration performed at all the measurement frequencies using a load impedance value close to that of the sample [21,23,25], assures that this increase is not an artifact due to electrode polarization. The strong conductivity increase at frequencies of the order of 1 MHz corresponds to the Maxwell–Wagner–O'Konski dispersion.

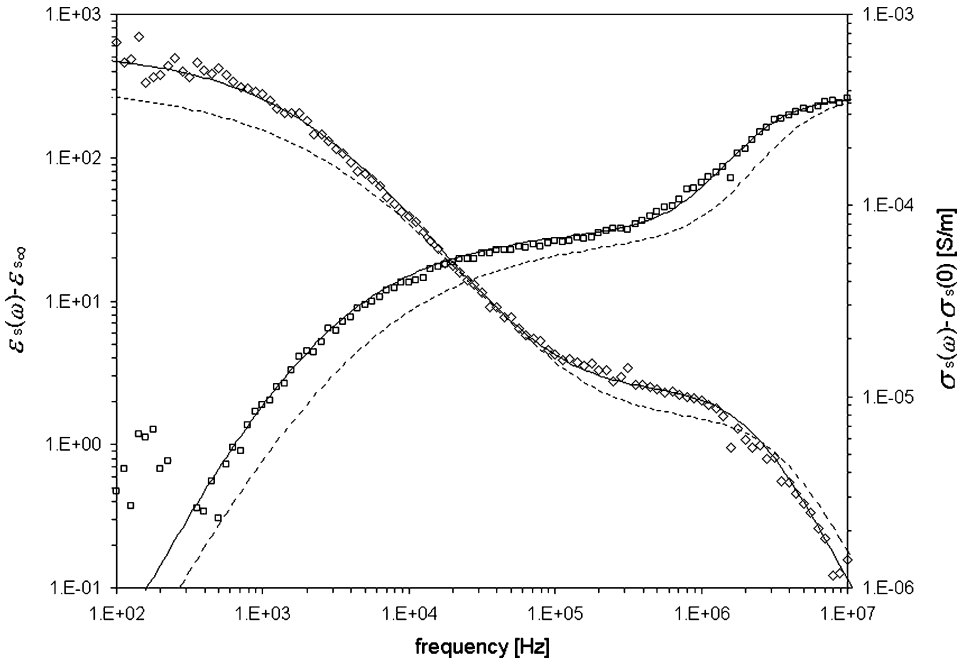

Fig. 4. As Fig. 2 but for a KCl electrolyte solution.

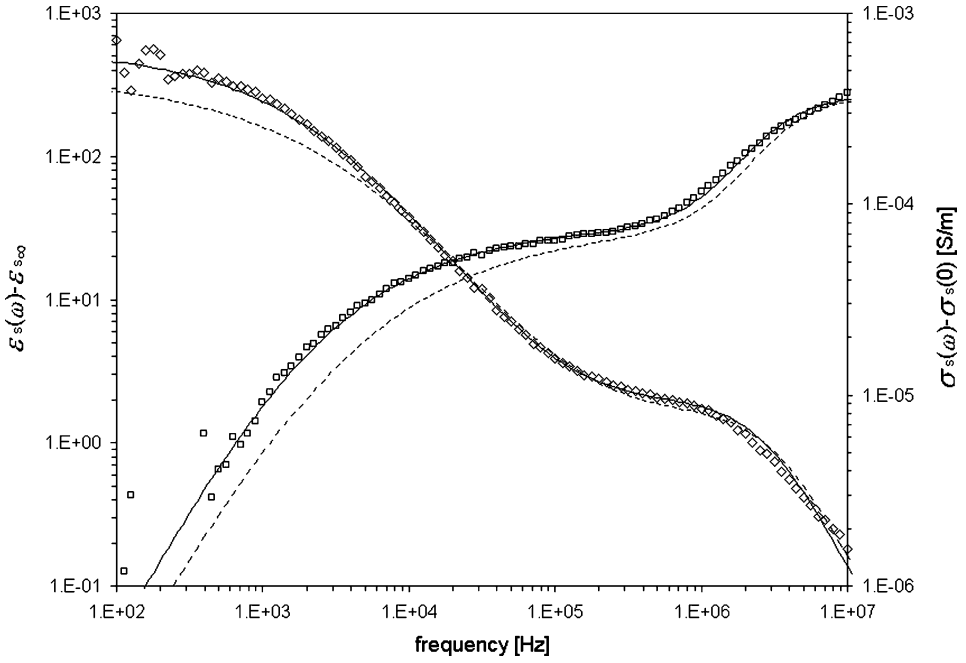

Fig. 5. As Fig. 2 but for a NaCl electrolyte solution.

3.1. Macroscopic dispersion parameters

In order to describe the experimental data we used the spectral function proposed by Nettelbalat–Niklasson [26] for the description of the LFDD, plus an additional high-frequency single time constant dispersion term:

$$\sigma_s(\omega) + i\omega\varepsilon_0\varepsilon_s(\omega) = \sigma_s(0) + i\omega\varepsilon_0\left[\phi\left(\frac{\delta\varepsilon_L}{1+\gamma\sqrt{i\omega\tau_L}+i\omega\tau_L} + \frac{\delta\varepsilon_H}{1+i\omega\tau_H}\right) + \varepsilon_{s\infty}\right]. \quad (2)$$

In this expression, the lower indexes L, and H refer to the low- and the high-frequency dispersions, $\delta\varepsilon_L$, τ_L, $\delta\varepsilon_H$, and τ_H, are the amplitudes and characteristic times of these dispersions, and γ is a dimensionless fitting parameter that has a value of the order of unity.

The fitting was performed taking care to ensure a perfect agreement for the high-frequency permittivity and the low-frequency conductivity, which is required for the logarithmic

Table 1
Measured (first two rows) and fitted parameter values. The ζ-potential values were deduced from measured electrophoretic mobility data using Eq. (16)

	KAc	NaAc	KCl	NaCl
pH	7.1	6.2	7.1	6.1
ζ (mV)	−202	−198	−206	−215
$\varepsilon_{s\infty}$	77.4	78.1	78.2	77.8
$\delta\varepsilon_L$ (10^4)	5.80	5.80	5.80	5.80
$\delta\varepsilon_H$	125	147	236	193
τ_L (10^{-5} s)	11.0	9.50	6.50	6.50
τ_H (10^{-8} s)	4.50	6.70	7.10	5.80
$\sigma_s(0)$ (10^{-3} S/m)	3.69	3.57	5.55	4.51
γ	1.27	1.48	1.39	1.54

representations. The obtained results are shown in Figs. 2–5, while the fitted values of the macroscopic parameters appear in Table 1. In view of the low sensitivity of the used spectral function, Eq. (2), to the value of the parameter γ, its value could not be directly determined given the precision of the experimental data. Therefore, the values of this parameter appearing in Table 1, and used in the fitting process of the remaining parameters, were calculated using the following expression, based on the theoretical model described below

$$\gamma = \sqrt{\frac{a^2}{D_{\mathrm{ef}}\tau_L}},$$

where

$$D_{\mathrm{ef}} = 2D^+D^-/\big(D^+ + D^-\big). \tag{3}$$

Table 1 also includes ζ-potential values deduced from measured electrophoretic mobility values u, using Eq. (16) [20]. These values correspond to the second, high ζ-potential, solution.

4. Analysis of the experimental data using a theoretical model

4.1. Theoretical model

In order to analyze the experimental results we used the Shilov–Dukhin model [8,27] for the low-frequency dielectric dispersion, combined with the Maxwell–Wagner–O'Konski model [28–30] for the high-frequency dispersion. This leads to the following frequency dependence of the dipolar coefficient of a suspended particle [17,31]

$$d^*(\omega) = d_L^*(\omega) + d_H^*(\omega),$$

where

$$d_L^*(\omega) = \frac{\delta d_L}{1 + \frac{i\omega\tau_L}{1+\sqrt{2/S}\sqrt{i\omega\tau_L}}},$$

$$d_H^*(\omega) = \frac{\delta d_H}{1 + i\omega\tau_H} + d_\infty. \tag{4}$$

For binary univalent electrolyte solutions, the analytical expressions for the dipolar coefficient parameters are

$$\delta d_L = -3\big(R^+ + R^-\big)H/(2B), \tag{5}$$

$$\tau_L = Sa^2/(2D_{\mathrm{ef}}), \tag{6}$$

$$S = A/B, \tag{7}$$

$$\delta d_H = \frac{Rel-2}{Rel+4} - d_\infty,$$

$$\tau_H = \frac{\varepsilon_0(\varepsilon_i + 2\varepsilon_e)}{2\sigma_e(Rel+1)}, \tag{8}$$

$$d_\infty = \frac{\varepsilon_i - \varepsilon_e}{\varepsilon_i + 2\varepsilon_e}, \tag{9}$$

where

$$R^\pm = \frac{2G_0^\pm}{aC_\infty} + 6m^\pm\left[\frac{G_0^\pm}{aC_\infty} \pm \frac{\tilde\zeta}{\kappa a}\right], \tag{10}$$

$$G_0^\pm = \frac{2C_\infty}{\kappa}\big(e^{\mp\tilde\zeta/2} - 1\big),$$

$$m^\pm = \frac{2\varepsilon_0\varepsilon_e}{3\eta D^\pm}\left(\frac{kT}{e}\right)^2,$$

$$H = \Big[\big(R^+ - R^-\big)\big(1-\Delta^2\big) - U^+ + U^- + \Delta\big(U^+ + U^-\big)\Big]\Big/A,$$

$$\Delta = \big(D^- - D^+\big)\big/\big(D^+ + D^-\big), \tag{11}$$

$$U^\pm = \frac{48m^\pm}{\kappa a}\ln\left(\cosh\frac{\tilde\zeta}{4}\right), \tag{12}$$

$$A = Rel + 4, \tag{13}$$

$$B = \big(R^+ + 2\big)\big(R^- + 2\big) - U^+ - U^- - \big(U^+R^- + U^-R^+\big)/2, \tag{14}$$

$$Rel = R^+ + R^- - \Delta\big(R^+ - R^-\big), \tag{15}$$

$$\tilde\zeta = \zeta/(kT),$$

and ε_i is the relative permittivity of the suspended particle.

The expression for the dipolar coefficient makes it possible to calculate the electrophoretic mobility of a suspended particle and the dielectric properties of the suspension. We could not use the well-known Dukhin–Semenikhin result [32] because it is limited to the case $D^+ = D^-$. We used, therefore, the expression for the electrophoretic mobility deduced in [20]

$$u = \frac{2\varepsilon_0\varepsilon_e\zeta}{3\eta}\left\{1 - \delta d_L - \delta d_H - d_\infty + \frac{\delta d_L}{H}\left[\Delta - \frac{4}{\tilde\zeta}\ln\left(\cosh\frac{\tilde\zeta}{4}\right)\right]\right\}. \tag{16}$$

The complex conductivity of the suspension was calculated using the Maxwell mixture formula

$$\sigma_s(\omega) + i\omega\varepsilon_0\varepsilon_s(\omega) = (\sigma_e + i\omega\varepsilon_0\varepsilon_e)\big\{1 + 3\phi d^*(\omega)\big\}.$$

Including, as usually done [31], just one low-frequency term in the permittivity and conductivity expressions

$$\varepsilon_s(\omega) = \varepsilon_e\left\{1 + 3\phi\left[\mathrm{Re}\big(d_H^*\big) + \frac{\sigma_e}{\omega\varepsilon_0\varepsilon_e}\,\mathrm{Im}\big(d_L^* + d_H^*\big)\right]\right\},$$

$$\sigma_s(\omega) = \sigma_e\left\{1 + 3\phi\left[\mathrm{Re}\big(d_L^* + d_H^*\big) - \frac{\omega\varepsilon_0\varepsilon_e}{\sigma_e}\,\mathrm{Im}\big(d_H^*\big)\right]\right\},$$

leads back to Eq. (2), with the following expressions for the macroscopic dispersion parameters

$$\sigma_s(0) = \sigma_e\big[1 + 3\phi(\delta d_L + \delta d_H + d_\infty)\big], \tag{17}$$

$$\delta\varepsilon_L = -3\sigma_e(\tau_L/\varepsilon_0)\delta d_L, \tag{18}$$

$$\delta\varepsilon_H = 3\sigma_e(\varepsilon_e/\sigma_e - \tau_H/\varepsilon_0)\delta d_H, \tag{19}$$

$$\varepsilon_{s\infty} = \varepsilon_e(1 + 3\phi d_\infty), \tag{20}$$

$$\gamma = \sqrt{2/S}. \tag{21}$$

It should be noted that the macroscopic and microscopic values of the characteristic times τ_L and τ_H coincide with one another.

Fig. 6 shows theoretical permittivity spectra calculated for the four considered electrolytes and for the following parameter values $C_\infty = 1.76 \times 10^{23}$ m^{-3}, $\varepsilon_e = 78.54$, $\varepsilon_i = 2$, and $\zeta = -210$ mV. The analytical results are compared to numerical data calculated using the Network Simulation Method [33]. As can be seen, there is a very good agreement in the whole frequency range, except for a slight discrepancy at low frequencies. In view of this agreement we used theoretical results for all the forthcoming analysis.

It should be noted that some of the curves in Fig. 6 overlap almost exactly so that only two pairs of curves seem to be visible. At low frequencies, the lowest pair corresponds to KAc and NaAc, while the highest pair corresponds to KCl and NaCl. On the contrary, at high frequencies, the lowest pair corresponds to NaAc and NaCl, while the highest pair to KAc and KCl. This means that, at least in the considered case of highly charged particles, theoretical and numerical results predict that the low-frequency dielectric dispersion is mainly determined by the diffusion coefficient of co-ions [16], while the diffusion coefficient of counterions determines the high-frequency dispersion.

This high-frequency behavior can be easily interpreted combining Eqs. (1), (8), (11), (15)

$$\tau_H = \frac{kT}{2e^2C_\infty}\frac{\varepsilon_0(\varepsilon_i + 2\varepsilon_e)}{(2R^+ + 1)D^+ + (2R^- + 1)D^-}. \tag{22}$$

This result shows that D^+ and D^- enter the expression of τ_H in a non-symmetric fashion. For highly charged particles, the diffusion coefficient of counterions is multiplied by a large factor (R^+ is large, Eq. (10)), while the diffusion coefficient of co-ions is multiplied by a factor that is close to one (R^- is small). Therefore, the second addend in the denominator of Eq. (22) becomes negligible as compared to the first showing that the characteristic time of the high-frequency dispersion is determined by the diffusion coefficient of counterions. This is a rather obvious conclusion since the high-frequency dispersion parameters depend on the surface conductivity of the particles, which is mainly determined by the mobility of the ions in the double layer (mostly counterions).

The interpretation of the low-frequency behavior is slightly less evident. We start calculating the parameter S, combining Eqs. (7), (11), (13)–(15)

$$S = \frac{4}{D^+ + D^-}\frac{(R^+ + 2)D^+ + (R^- + 2)D^-}{(R^- + 2)(R^+ + 2 - U^+) + (R^+ + 2)(R^- + 2 - U^-)}.$$

In this expression, the addends $U^\pm$, Eq. (12), which are related to the convective flow of ions in the double layer, are relatively small so that they can be neglected leading to

$$S \approx \frac{2}{D^+ + D^-}\frac{(R^+ + 2)D^+ + (R^- + 2)D^-}{(R^- + 2)(R^+ + 2)}.$$

Combining this result with Eq. (6) and canceling the D_{ef} factor, Eq. (3), finally gives

$$\tau_L \approx \left[\frac{1}{(R^+ + 2)D^+} + \frac{1}{(R^- + 2)D^-}\right]\frac{a^2}{2}. \tag{23}$$

Just as in the preceding case, the diffusion coefficient values D^+ and D^- enter the expression of the characteristic time in

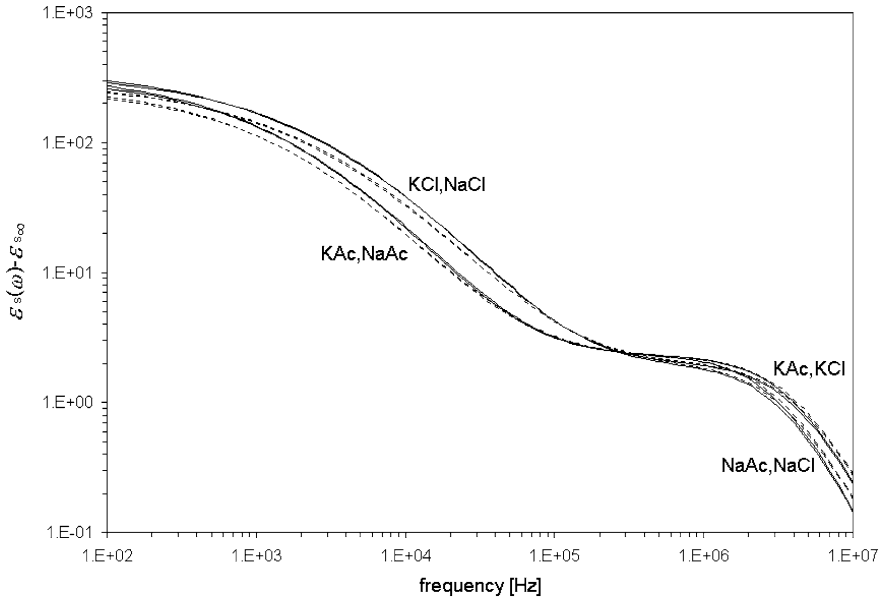

Fig. 6. Theoretical (dashed lines) and numerical (solid lines) permittivity spectra for suspensions of the indicated aqueous electrolyte solutions.

a non-symmetric fashion. For highly charged particles, the diffusion coefficient of counterions is multiplied by a large factor while the diffusion coefficient of co-ions is multiplied by a factor that is close to two. Therefore, the first addend in Eq. (23) becomes negligible as compared to the second showing that the characteristic time of the low-frequency dispersion is determined by the diffusion coefficient of co-ions.

It should be noted that the analytical expression used to define τ_L, Eq. (6), is not obvious. Actually, the original definition [8,27] does not include the parameter S

$$\tau_{L,\mathrm{ori}} = \frac{a^2}{2D_{\mathrm{ef}}} \tag{24}$$

so that the expression for the dipolar coefficient has also a different form

$$d^*_{L,\mathrm{ori}}(\omega) = \frac{\delta d_L}{1 + \frac{i\omega S\tau_{L,\mathrm{ori}}}{1+\sqrt{2}\sqrt{i\omega\tau_{L,\mathrm{ori}}}}}.$$

However, Fig. 6 shows that the used definition, Eq. (6), seems to be preferable to the original one, Eq. (24), since, in the latter, the diffusion coefficients of counterions and co-ions enter in a fully symmetric fashion, Eq. (3).

4.2. Theoretical predictions

In order to calculate the permittivity and conductivity spectra predicted by the theory it is necessary to first determine the values of all the parameters defining the model. For each suspension this was done as follows:

1. Equations (9) and (20) were combined with the fitted value of $\varepsilon_{s\infty}$, Table 1, and the value $\varepsilon_i = 2$, to give the permittivity of the suspending medium ε_e. This forced the theoretical and fitted permittivity spectra to coincide at high frequencies, making it possible to include the theoretical results in Figs. 2–5.
2. The conductivity σ_e of the suspending medium was adjusted so that the theoretical value of the limiting low-frequency conductivity, Eq. (17), reproduced the corresponding fitted value, Table 1. Again, this made it possible to include the theoretical conductivity results in Figs. 2–5. The value of the conductivity was used to calculate the ion concentrations C_∞, Eq. (1).
3. We first tried to adjust the ζ-potential in such a way as to make $\delta\varepsilon_L$, Eq. (18), coincide with the value deduced from the experimental data, Table 1. This proved to be impossible since the fitted values of $\delta\varepsilon_L$ were always much higher than the maximum predicted by the theory (Eqs. (5), (6), (18) with $\zeta \to -\infty$). Therefore, the ζ-potential values were adjusted to best reproduce the high-frequency dispersion parameters. This was done by forcing the theoretical value of the limiting high-frequency conductivity

$$\sigma_{s\infty} = \sigma_e + 3\phi\left(\sigma_e d_\infty + \frac{\varepsilon_0\varepsilon_e\delta d_H}{\tau_H}\right)$$

which has the advantage of being a function of both the amplitude and the characteristic time of the high-frequency dispersion, to coincide with the value deduced from the experimental data:

$$\sigma_{s\infty} = \sigma_s(0) + \phi\varepsilon_0\left(\frac{\delta\varepsilon_L}{\tau_L} + \frac{\delta\varepsilon_H}{\tau_H}\right).$$

Table 2
Model parameters (first three lines) and theoretical predictions

	KAc	NaAc	KCl	NaCl
ε_e	78.5	79.3	79.4	78.9
σ_e (10^{-3} S/m)	3.66	3.55	5.54	4.52
ζ (mV)	−185	−184	−193	−202
$\delta\varepsilon_L$ (10^4)	2.65	3.28	3.23	3.55
$\delta\varepsilon_H$	169	158	152	164
τ_L (10^{-5} s)	6.95	7.31	4.01	4.11
τ_H (10^{-8} s)	5.77	6.54	4.36	4.88
γ	1.60	1.69	1.77	1.94

The ζ-potential values were deduced from high-frequency dielectric dispersion data, see text.

The theoretical model and parameter values so obtained appear in Table 2, while the theoretical curves are shown in Figs. 2–5.

5. Discussion

The aim of this study was to analyze the dependence of the low- and high-frequency dielectric spectra of latex suspensions on the difference of the counterion and co-ion diffusion coefficients. This was done considering four different electrolytes (KAc, NaAc, KCl, and NaCl) and comparing measured dielectric data with theoretical and numerical predictions.

The experimental data was fitted using the Nettelblad–Niklasson [26] expression, which allows a direct comparison with the theoretical predictions of the Shilov–Dukhin model [8,27], since this model leads to the same spectral function for the dielectric spectrum. This function of frequency proved to be satisfactory for the description of the permittivity and conductivity data using 7 adjustable parameters, Figs. 2–5 and Table 1. We actually used only 6 free parameters, expressing the seventh in terms of the characteristic time of the low-frequency dielectric dispersion, the ion diffusion coefficients, and the particle radius.

The main qualitative conclusion drawn from the theory for the considered case of highly charged particle suspensions (both analytical expressions and numerical calculations), is that the low-frequency dispersion parameters should depend on the diffusion coefficient of co-ions, while the high-frequency dispersion is dependent on the diffusion coefficient of counterions, Fig. 6. This behavior is partly reproduced by our experimental results, Table 1 and Fig. 7, which shows in a single plot all the experimental results. Clearly, the low-frequency behavior is mainly determined by the diffusion coefficient of co-ions. However, there seems to be no evidence on the dependence of the high-frequency dispersion on the diffusion coefficient of counterions.

The reason for this disagreement is most likely of experimental nature. The measurement cell used in this study was de-

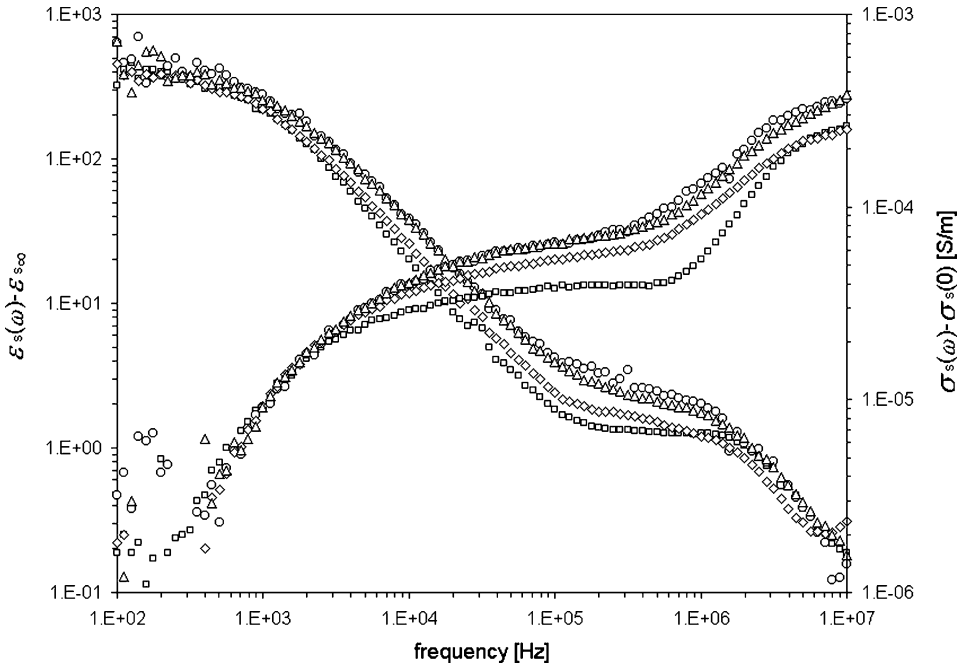

Fig. 7. Experimental permittivity (declining curves) and conductivity (rising curves) spectra for suspensions of latex particles in KAc (squares), NaAc (diamonds), KCl (circles), and NaCl (triangles), aqueous electrolyte solutions.

signed to optimize low-frequency measurements: angular frequencies well below the relaxation frequency of the electrolyte solution $\sigma_e/(\varepsilon_0\varepsilon_e)$. Under these conditions, the main problem to overcome is that of the electrode polarization. However, at high frequencies, the main difficulty is that of the stray field surrounding the cell. We tried to overcome this last problem by reducing to a minimum the range of spacings used in the measurements: electrode separations of 1–3 mm for a 15 mm electrode diameter. Apparently this was not sufficient to determine with acceptable precision the parameters of the tiny high-frequency dispersion (dispersion amplitude of the order of one dielectric unit for a 1% particle concentration).

For the considered suspensions, the theoretical predictions lead to characteristic time values of the low-frequency dispersion, that are acceptably close to the experimental ones, Tables 1 and 2. More important, all these values are in qualitative agreement in what respects to their dependence on the diffusion coefficients: they markedly increase with decreasing mobility of co-ions and are little dependent on the mobility of counterions. In the case of the theoretical values, this behavior is only obtained for the definition of τ_L given in Eq. (6), since the original definition, Eq. (24), is totally symmetric with respect to the diffusion coefficients of counterions and co-ions.

As for the low-frequency dispersion amplitudes, the theoretical predictions lead to values that are much smaller than the experimental ones, Tables 1 and 2. This discrepancy, which was often reported in the literature [2,3,7], cannot be overcome with an appropriate choice of the ζ-potential in the theoretical model. It stems from a still elusive inadequacy of the standard electrokinetic model to represent the considered system (extended models including an anomalous surface conductivity [34,35] are often still inadequate).

Finally, despite the probable lack of precision of the high-frequency dielectric dispersion data, this data could be fairly well reproduced by theoretical results using ζ-potential values that were compatible with those deduced from electrophoretic measurements, Tables 1 and 2. This suggests that the standard electrokinetic model was adequate for the representation of the surface conductivity [36,37], so that the anomalous or stagnant layer conductivity is relatively small in the considered systems [38].

Acknowledgments

Financial support by the Consejo de Investigaciones de la Universidad Nacional de Tucumán (26/E220), Agencia Nacional de Promoción Científica y Tecnológica (PICT 03/8668), and Consejo Nacional de Investigaciones Científicas y Técnicas (PIP 0465/98) of Argentina are gratefully acknowledged. We are grateful to F. González-Caballero and A. Delgado for allowing us to make the electrophoretic mobility measurements at the University of Granada, Spain, with the help of S. Ahualli, and to J.J. López-García, University of Jaén, Spain, for performing the numerical calculations.

References

[1] H.P. Schwan, G. Schwarz, J. Maczuk, H. Pauly, J. Phys. Chem. 66 (1962) 2626.
[2] M.M. Springer, A. Korteweg, J. Lyklema, J. Electroanal. Chem. 153 (1983) 55.
[3] D.E. Dunstan, L.R. White, J. Colloid Interface Sci. 152 (1992) 308.
[4] F. Carrique, L. Zurita, A.V. Delgado, J. Colloid Interface Sci. 166 (1994) 128.
[5] M.R. Gittings, D.A. Saville, Langmuir 11 (1995) 798.
[6] G. Blum, H. Maier, F. Sauer, H.P. Schwan, J. Phys. Chem. 99 (1995) 780.

[7] C. Grosse, M. Tirado, W. Pieper, R. Pottel, J. Colloid Interface Sci. 205 (1998) 26.
[8] S.S. Dukhin, V.N. Shilov, Dielectric Phenomena and the Double Layer in Disperse Systems and Polyelectrolytes, Kerter Publishing House, Jerusalem, 1974.
[9] R.W. O'Brien, Adv. Colloid Interface Sci. 16 (1982) 281.
[10] J. Lyklema, S.S. Dukhin, V.N. Shilov, J. Electroanal. Chem. 143 (1983) 1.
[11] M. Fixman, J. Chem. Phys. 78 (1983) 1483.
[12] C. Grosse, K.R. Foster, J. Phys. Chem. 91 (1987) 3073.
[13] E.H.B. DeLacey, L.R. White, J. Chem. Soc. Faraday Trans. 2 77 (1981) 2007.
[14] C.S. Mangelsdorf, L.R. White, J. Chem. Soc. Faraday Trans. 2 93 (1997) 3145.
[15] J.J. López-García, J. Horno, A.V. Delgado, F. González-Caballero, J. Phys. Chem. B 103 (1999) 11297.
[16] F.J. Arroyo, A.V. Delgado, F. Carrique, M.L. Jiménez, T. Bellini, F.J. Mantegazza, Chem. Phys. 114 (2002) 10973.
[17] V.N. Shilov, A.V. Delgado, F. González-Caballero, C. Grosse, Colloids Surf. A 192 (2001) 253.
[18] C. Grosse, J.J. López-García, J. Horno, J. Phys. Chem. B 108 (2004) 8397.
[19] J.J. López-García, C. Grosse, J. Horno, J. Phys. Chem. B 109 (2005) 5808.
[20] J.J. López-García, C. Grosse, J. Horno, J. Phys. Chem. B 109 (2005) 11907.
[21] M.C. Tirado, F.J. Arroyo, A.V. Delgado, C. Grosse, J. Colloid Interface Sci. 227 (2000) 141.
[22] M. Honda, The Impedance Measurement Handbook: A Guide to Measurement Technology and Techniques, Hewlett–Packard, Yokogawa, Japan, 1989.
[23] C. Grosse, M. Tirado, IEEE Trans. Instrumentation and Measurement 50 (2001) 1329.
[24] H.P. Schwan, in: W.L. Nastuk (Ed.), Physical Techniques in Biological Research, vol. 6, Academic Press, New York, 1963.
[25] C. Grosse, M. Tirado, Mater. Res. Soc. Proc. 430 (1996) 287.
[26] B. Nettelblad, G.A. Niklasson, J. Colloid Interface Sci. 181 (1996) 165.
[27] C. Grosse, V.N. Shilov, J. Phys. Chem. 100 (1996) 1771.
[28] J.C. Maxwell, Electricity and Magnetism, vol. 1, Clarendon, Oxford, 1892.
[29] K.W. Wagner, Arch. Elektrotech. 2 (1914) 371.
[30] C.T. O'Konski, J. Phys. Chem. 64 (1960) 605.
[31] C. Crosse, F.J. Arroyo, V.N. Shilov, A.V. Delgado, J. Colloid Interface Sci. 242 (2001) 75.
[32] S.S. Dukhin, N.M. Semenikhin, Koll. Zhur. 32 (1970) 366.
[33] J. Horno (Ed.), Network Simulation Method, Research Signpost, Trivandrum, 2002.
[34] C.F. Zukoski, D.A. Saville, J. Colloid Interface Sci. 114 (1986) 32.
[35] M. Minor, A. van der Wal, J. Lyklema, in: E. Pelizetti (Ed.), Fine Particles Science and Technology, Kluwer Academic, The Netherlands, 1996.
[36] J.J. Bikerman, Z. Physik. Chem. 163 (1933) 378.
[37] J.J. Bikerman, Kolloid Z. 72 (1935) 100.
[38] A.S. Russel, P.J. Scales, C.S. Mangelsdorf, L.R. White, Langmuir 11 (1995) 1553.